Video Article

Graphene Coatings for Biomedical Implants

Ramakrishna Podila[1,2], Thomas Moore[3], Frank Alexis[3], Apparao Rao[1,4]

[1]Department of Physics, Clemson University

[2]Department of Pharmacology and Toxicology, East Carolina University

[3]Department of Bioengineering, Clemson University

[4]Center for Optical Materials Science and Engineering Technologies, Clemson University

Correspondence to: Apparao Rao at arao@clemson.edu

URL: https://www.jove.com/video/50276
DOI: doi:10.3791/50276

Keywords: Biomedical Engineering, Issue 73, Bioengineering, Medicine, Biophysics, Materials Science, Physics, Pharmacology, Toxicology, Surgery, Chemistry and Materials (General), graphene, biomedical implants, surface modification, chemical vapor deposition, protein expression, confocal microscopy, implants, stents, clinical

Date Published: 3/1/2013

Citation: Podila, R., Moore, T., Alexis, F., Rao, A. Graphene Coatings for Biomedical Implants. *J. Vis. Exp.* (73), e50276, doi:10.3791/50276 (2013).

Abstract

Atomically smooth graphene as a surface coating has potential to improve implant properties. This demonstrates a method for coating nitinol alloys with nanometer thick layers of graphene for applications as a stent material. Graphene was grown on copper substrates *via* chemical vapor deposition and then transferred onto nitinol substrates. In order to understand how the graphene coating could change biological response, cell viability of rat aortic endothelial cells and rat aortic smooth muscle cells was investigated. Moreover, the effect of graphene-coatings on cell adhesion and morphology was examined with fluorescent confocal microscopy. Cells were stained for actin and nuclei, and there were noticeable differences between pristine nitinol samples compared to graphene-coated samples. Total actin expression from rat aortic smooth muscle cells was found using western blot. Protein adsorption characteristics, an indicator for potential thrombogenicity, were determined for serum albumin and fibrinogen with gel electrophoresis. Moreover, the transfer of charge from fibrinogen to substrate was deduced using Raman spectroscopy. It was found that graphene coating on nitinol substrates met the functional requirements for a stent material and improved the biological response compared to uncoated nitinol. Thus, graphene-coated nitinol is a viable candidate for a stent material.

Video Link

The video component of this article can be found at https://www.jove.com/video/50276/

Introduction

The past three decades have witnessed discovery of novel materials-based therapies and devices for disease treatments and diagnostics. Novel alloy materials such as nitinol (NiTi) and stainless steel are often used in biomedical implant manufacturing due to their superior mechanical properties.[1-3] However, numerous challenges remain due to exogenous material cytotoxicity, bio- and hemo-compatibility. The metallic nature of these alloys results in poor bio- and hemocompatibility due to metal leaching, lack of cell adhesion, proliferation, and thrombosis when it comes in contact with flowing blood (such as catheters, blood vessel grafts, vascular stents, artificial heart valves *etc.*). [1, 4, 5] The interaction of proteins or living cells with the implant surface can lead to a strong immunological response and the ensuing cascade of biochemical reactions may adversely affect the device functionality. Therefore, it is pertinent to achieve control over the interactions between biomedical implants and its surrounding biological environment. Surface modification is often employed to reduce or prevent the adverse physiological response originating from the implant material. An ideal surface coating is expected to have high adhesion strength, chemical inertness, high smoothness, and good hemo- and biocompatibility. Previously, numerous materials including diamond-like carbon (DLC), SiC, TiN, TiO_2 and many polymer materials have been tested as bio-compatible implant surface coatings. [1, 6-23] However, these materials are still unable to meet all of the functional criteria for a suitable implant surface coating.

The discovery of atom thick layer of sp^2 carbon, known as graphene, has opened doors for the development of novel multifunctional materials. Graphene is expected to be an ideal candidate for implant surface coating since it is chemically inert, atomically smooth and highly durable. In this Letter, we investigate the viability of graphene as a surface coating for biomedical implants. Our studies show that the graphene coated nitinol (Gr-NiTi) meets all of the functional criteria, and additionally supports excellent smooth muscle and endothelial cell growth leading to better cell proliferation. We also find that the serum albumin adsorption on Gr-NiTi is higher than fibrinogen. Importantly, (i) our detailed spectroscopic measurements confirmed the lack of charge transfer between graphene and fibrinogen suggesting that graphene coating inhibits platelet activation by implants, (ii) graphene coatings do not exhibit any significant *in vitro* toxicity for endothelial and smooth muscle cell lines confirming their biocompatibility, and (iii) graphene coatings are chemically inert, durable and impermeable in flowing blood environment. These hemo-and biocompatible properties, along with high strength, chemical inertness and durability, render graphene coatings as an ideal surface coating.

Protocol

1. Graphene-coating of NiTi

1. The graphene samples used in this study were grown on copper (Cu) substrates using the chemical vapor deposition technique, and subsequently transferred to 4.5 mm^2NiTi substrates.
2. Cu foils (1 cm x 1 cm) were placed in a 1 in. quartz tube furnace and heated to 1,000 °C in the presence of 50 sccm of H_2 and 450 sccm of Ar.
3. Next, methane (1 and 4 sccm) was introduced into the furnace at different flow rates for 20-30 min. The samples were finally cooled to room temperature under flowing H_2, Ar and CH_4.
4. Next, the Cu foils were spin-coated with PMMA (diluted with 4% anisole) at 4,000 rpm followed by a heat treatment for 5 min at 150 °C. Graphene attached to PMMA layer was obtained by etching the Cu foil using Transene Inc., CE-100 etchant, and subsequent rinsing in 10% HCl and de-ionized water for 10 min.
5. The samples were transferred to NiTi substrates (4.5 mm^2) and annealed at 450 °C in Ar (300 sccm) and H_2 (700 sccm) for 2 hr to remove the PMMA. Finally, the substrates were washed with acetone to dissolve the residual PMMA to obtain the Gr-NiTi sample. A Dilor XY triple grating monochromator was used for the micro-Raman characterization (using 100X objective) of all Gr-NiTisamples with the 514.5 nm excitation from an Ar^+ ion laser.

2. *In Vitro* Toxicity of Gr-NiTi

Rat aortic endothelial cells (Cell application Inc.,) were cultured on a gelatin coated 8 chambers slide. For testing the cell growth, pristine and Gr-NiTisubstrates were placed in wells without any gelatin coating. Scanning electron microscopy images were obtained using a Hitachi S-4800 SEM. Additionally, rat aortic smooth muscle cells were also grown in CellBind 96-well plates as a control group (Corning) in Dulbecco's Modified Eagle Medium (ATCC).

1. For testing cell viability, cells (both endothelial and smooth muscle cells) were seeded at 10^5 cells/well in wells containing pristine NiTi, 1 sccm or 4 sccm Gr-NiTi substrates, where the stated sccm corresponds to the methane flow used in the CVD growth of graphene. Cells were grown for the desired time period in an incubator at 37 °C and 5% CO_2, exchanging media every other day.
2. At the end time point, media was removed and fresh media containing 0.5 mg/ml thiazolyl blue tetrazolium bromide (or MTT obtained from Sigma) was added to each well. Cells were then incubated for an additional 3 hr. For the MTS assay, media was removed at the final time point and replaced with 120 µl of MTS working solution (Cell Tier 96 aqueous, Promega) and incubated for 3 hr.
3. Next, media was gently removed and 100 ml of dimethylsulfoxide (Sigma) was added to each well. After allowing 10 min for the MTT crystals to dissolve, the solution was transferred to another well plate. For the MTS assay, no dimethylsulfoxide was added to the wells. Well contents were moved to a new plate.
4. Absorbance was read at 490 nm and the percent viability was determined by normalizing absorbance to the average absorbance of the pristine NiTi sample. At least five repeats were done for each sample type.

3. Confocal Microscopy Studies of Cell Morphology

1. For confocal imaging of rat aortic smooth muscle cells, substrates were placed in an 8-chamber slide (Thermo Scientific). The cells were seeded at 25,000 cells/chamber and incubated for 3 days at 37 °C and 5% CO_2.
2. Cells were fixed on the substrate with 4% formaldehyde in phosphate buffered saline for 20 min.
3. Permeabilized with 0.1% Triton-X for 1 min.
4. Actin was stained with Alexa Fluor 488 phalloidin (Life Technologies). 100 µl of alexafluor 488 phalloidin at 200 units/ml in methanol was added to 1.9 ml of phosphate buffered saline. Cells were stained with 250 µl of alexafluor 488 phalloidin for 45 min and then washed twice with phosphate buffered saline.
5. Nuclei were mounted with VectaShield fluorescent mounting medium containing DAPI (Vector Laboratories). Confocal images were collected using a Nikon Confocal TI. A chamber seeded with cells without any substrate was used as a control.

4. Protein Adsorption Studies

1. Substrate dimensions were measured with calipers before starting the protein adsorption experiments. Three measurements were taken for each side of the approximately square samples and averaged to get the length and width.
2. Each sample, pristine NiTi, 1sccm and 4sccm Gr-NiTiwere incubated with 1 mg/ml albumin in phosphate buffered saline (PBS) or 1 mg/ml fibrinogen in PBS at room temperature for 3 hr.
3. Alike samples were combined in a microcentrifuge tube with 200 µl of reducing sample buffer and boiled for 5 min.
4. Samples were then diluted in a Tris/Glycine/SDS buffer (Bio-Rad) and run through a 4-15% Tris polyacrylamide electrophoresis gel (Bio-Rad) at 90 V for 100 min.
5. Gels were then stained with SYPRO Red. Dilute SYPRO Red (Life Technologies) stock solution at 1:5,000 in 7.5 v/v% acetic acid. Stain gels for 60 min.
6. Image gels using a Flourchem SP (Alpha Innotech).Fluorescent intensity was quantified using ImageJ software. Fluorescent intensity from each sample was normalized by the total area of substrate and fibrinogen adsorption was compared to albumin adsorption.

5. Western Blotting for Protein Expression

1. Western blot was performed to analyze total actin in rat aortic smooth muscle cells. Cells were seeded at 10,000 cells/substrate in a 96-well plate.
2. Cells were grown for three days before removing media. Total protein was extracted using RIPA buffer and a standard BCA assay (Lamda) was performed to quantify total protein.
3. Samples were diluted to the same concentration in RIPA and then boiled in a reducing sample buffer for 5 min.
4. Proteins were separated by a 4-15% Tris polyacrylamide gel *via* electrophoresis at 90 V for 100 min. A kaleidoscope protein standard (Bio-Rad) was used to assess protein molecular weight.
5. Proteins were transferred to a PVDF membrane and blocked with a 1% non-fat dry milk (Bio-Rad) solution.
6. Total actin was tagged with a rabbit anti-rat actin antibody (Sigma). A BM chemiluminescent kit (Roche) was used to detect the primary antibody. Membranes were imaged using FlourChem SP imaging equipment and fluorescent intensity was measured using ImageJ software. Fluorescent intensity was normalized by comparing to the pristine NiTisample.

Representative Results

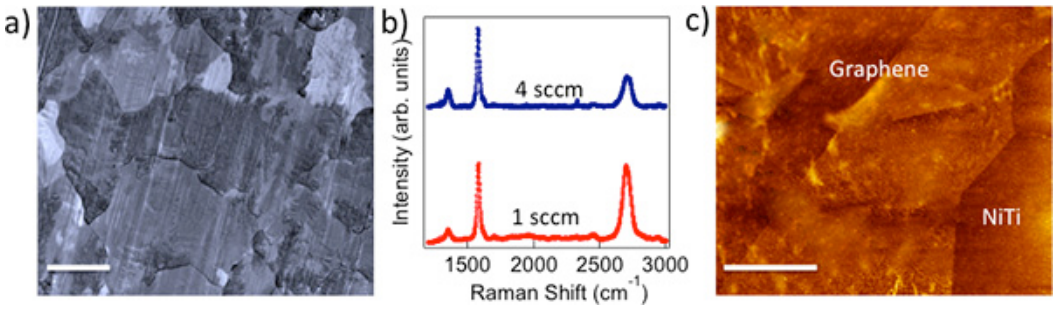

Figure 1. a) CVD grown polycrystalline graphene on Cu foils mimics the metal crystal grains (scale bar: 10 μm). b) Raman spectrum of 1 sccm (4 sccm) graphene shows intense (relatively weaker) G' band indicating monolayer (few layer) nature of as-prepared graphene. c) AFM image of graphene transferred on to NiTi shows a roughness of ~5 nm. Scale bar = 500 nm.

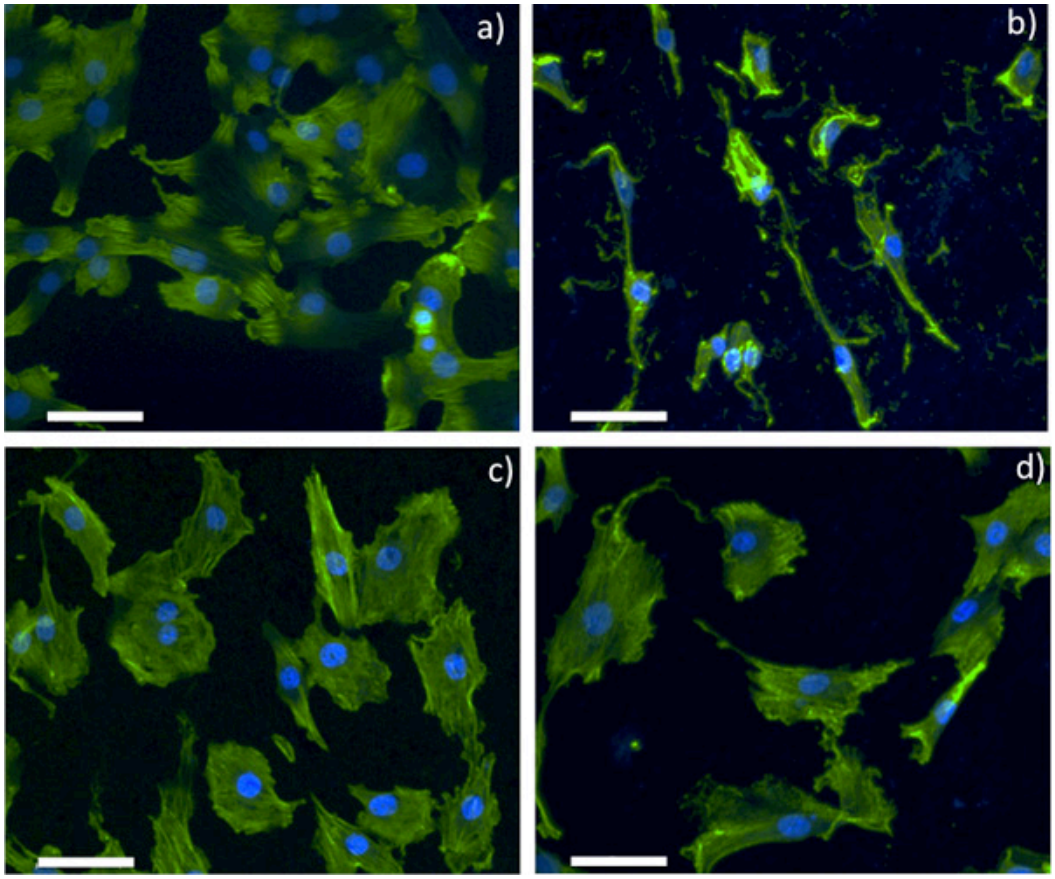

Figure 2. Confocal optical microscopy images for SMCs grown on **a)** control glass slide, **b)** pristine NiTi, **c)** 1 sccm Gr-NiTi and **d)** 4 sccm Gr-NiTi substrates (scale bar: 50 μm).

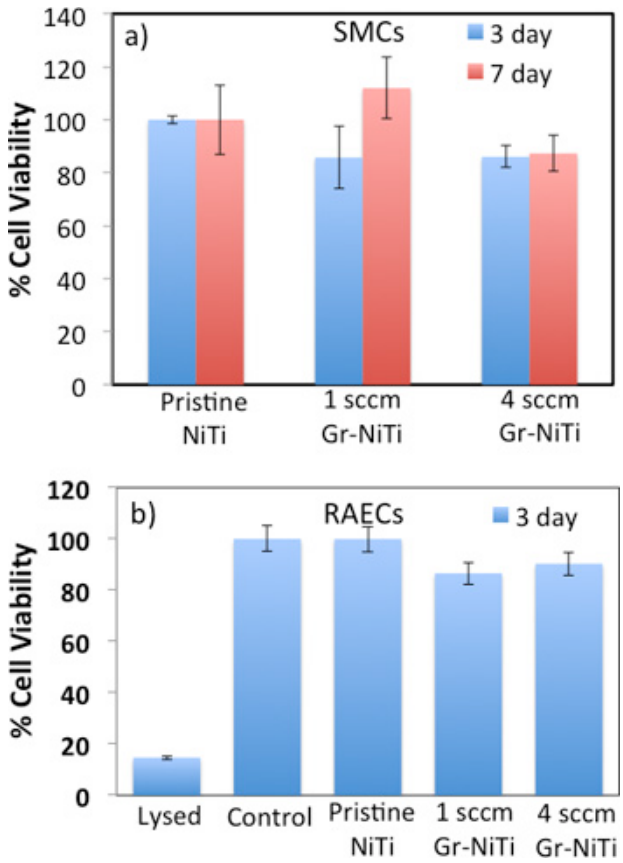

Figure 3. **a)** MTT assay shows that Gr-NiTi substrates (1 and 4 sccm) do not exhibit a significant difference in SMC cell viability relative to pristine NiTi. **b)** MTS assay shows that the 3 day cell viability for RAECs was not significantly different than controls.

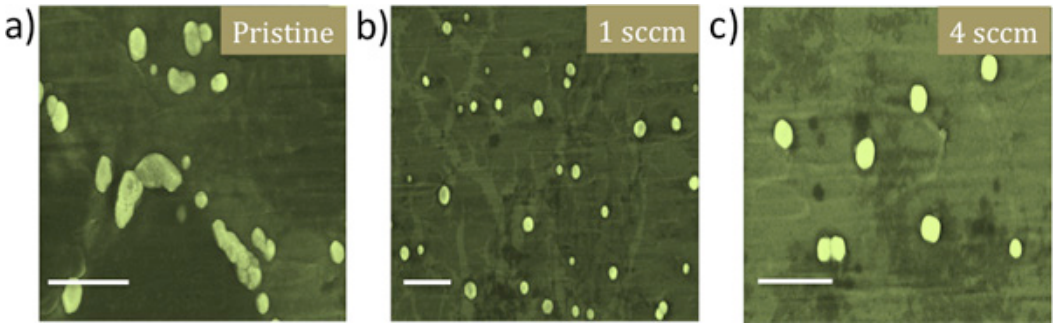

Figure 4. Scanning electron microscopy images for RAECs grown **a)** pristine NiTi, **b)** 1 sccm Gr-NiTi and **c)** 4 sccm Gr-NiTi substrates show that graphene coatings lead to better spherical cell morphology of RAECs. Scale bar = 10 μm.

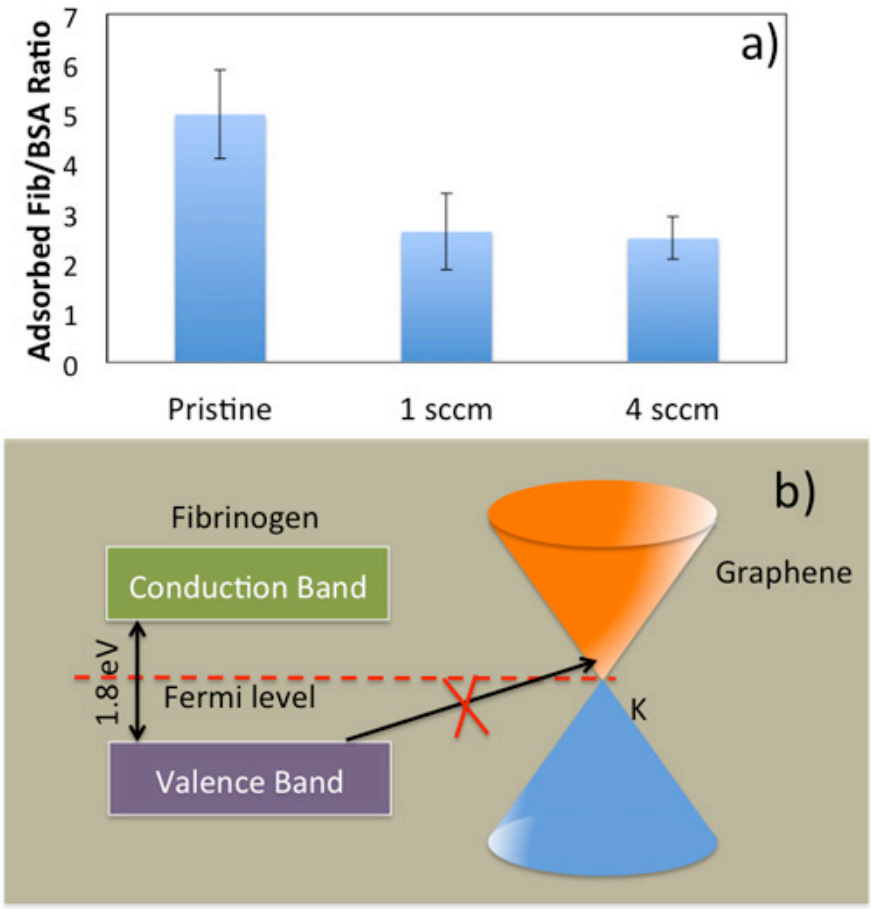

Figure 5. a) Fibrinogen/Albumin ratio for pristine NiTi, Gr-NiTi (1 and 4 sccm samples). **b)** Energy level diagram for fibrinogen and electronic density of states for graphene showing the equilibration of the Fermi level. An electron transfer from fibrinogen to Gr-NiTi is only possible from the occupied electronic states of the fibrinogen molecule into empty electronic states of Gr-NiTi at the same energy level. Both single- and few-layer graphene are semi-metals at room temperature with low density of states at *EF* which results in a weak (as compared to bare nitinol) charge transfer from fibrinogen to graphene.

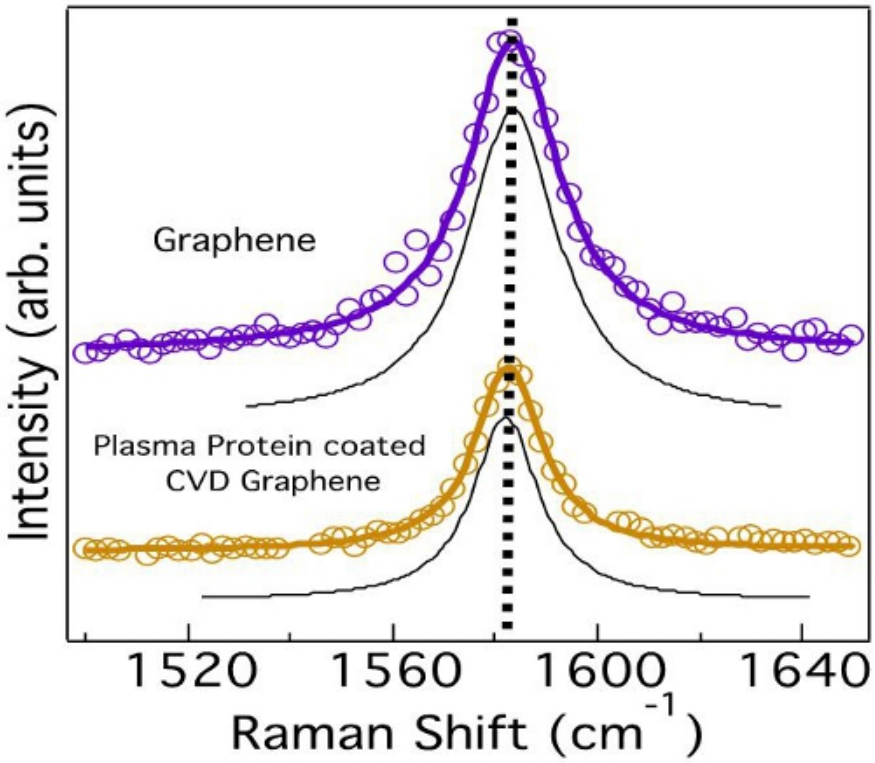

Figure 6. Graphene does not exhibit any changes in the G-band lineshape or frequency indicating the absence of any charge transfer from the plasma proteins. The deconvoluted peaks obtained from curve fitting are shown in black.

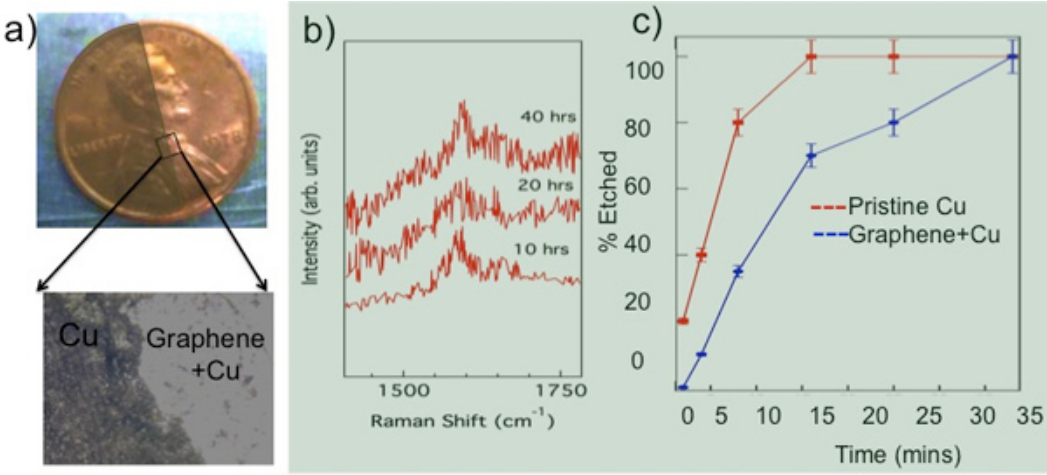

Figure 7. a) Graphene coated part of a Cu penny exposed to 5% H_2O_2 stays unchanged while the uncovered part is discolored. **b)** No change in the G-band frequency was observed in our *in situ* Raman studies of Gr-NiTi immersed in 70% HNO_3 confirming the durability of graphene coatings. **c)** The etch time for Cu in CE 100 solvent is doubled when Cu is coated with graphene (as in Gr-NiTi) indicating the impermeability of graphene membranes.

Discussion

Biocompatibility and cytotoxicity: The chemical vapor deposition (CVD) method yielded polycrystalline graphene samples that mimicked Cu crystal grains, as shown in **Figure 1a**. We employed Raman spectroscopy to confirm the presence of monolayer (few layer) graphene on 1 sccm (4 sccm) samples (see **Figure 1b**). Clearly, 1 sccm (4 sccm) samples exhibit intense (relatively weaker) G' band indicative of monolayer (few layer) graphene. **Figure 1c** shows an atomic force microscopy (AFM) image of few layer graphene on NiTi substrates. Our detailed measurements yielded a value of surface roughness R_q = 5 nm for transferred graphene layers (Gr-NiTi). It is well known that the nanostructured surface topography strongly affects cell shape and cytoskeletal assembly in endothelial cells and smooth-muscle cells. These cell lines respond to the mechanical stresses by changing their lipid-bilayer fluidity, which may adversely affect protein translocation and the entry of activators such as calcium into cells. More importantly, an increase in the cell membrane stress gradient can change conformation and density of cell surface

receptors. In order to test the influence of graphene coating on the stress gradients of cells, we studied the smooth muscle and endothelial cell morphology using microscopy techniques.

As shown in **Figure 2**, smooth muscle cell (SMC) morphology on pristine NiTi is non-spherical. Further, the cells are sparsely spread indicating weak adhesion of SMCs to the pristine NiTi. On the contrary, SMCs are dense and spherical on the Gr-NiTi (both 1 and 4 sccm) surfaces similar to the control. Graphene coating reduces stress gradients in the cells by providing smoother surfaces (evident from low R_q values shown in **Figure 1c**) and therefore results in a better cell morphology. In order to measure the cell viability and proliferation, we performed MTT assay on the SMCs grown on pristine and Gr-NiTisubstrates at 3 and 7 day time points. In this assay, the MTT dye (yellow color) is reduced into formazan dye (purple color) by the active reductase enzymes and therefore the healthy and proliferating cells (or the material's cytotoxicity) may be quantified by performing colorimetric measurements. As shown in **Figure 3a**, we did not observe any significant changes in toxicity for Gr-NiTi substrates after 3 and 7 days. These results confirm that the graphene coatings do not induce excess toxicity compared to the pristine NiTi substrates themselves.

To reconfirm the effects of graphene coating, we performed detailed electron microscopy imaging experiments on rat-aortic endothelial cells (see **Figure 4**). The cells on pristine NiTi substrates are sparse and elongated while they are ellipsoidal and dense on the Gr-NiTi substrates. Such improved cell morphology and density was found to be akin to SMCs confirming the reduction in stress gradients provided by the graphene coating. Further, we measured graphene coating cytotoxicity on RAEC using MTS 3-(4,5-dimethylthiazol-2-yl)-5-(3-carboxymethoxyphenyl)-2-(4-sulfophenyl)-2H-tetrazolium assay. The rationale for using MTS assay (instead of MTT) lies in its better compatibility with the RAEC growth media and conditions. As shown in **Figure 3b**, our MTS assay on the endothelial cell exhibited very good cell viability and proliferation confirming no excess toxicity from the graphene coatings even for RAEC. Importantly, both 1 and 4 sccm Gr-NiTi exhibited no significant changes in cell proliferation suggesting no dependence of the cell morphology upon number of graphene layers.

Protein Adsorption and Hemocompatibility: Blood clotting in the vicinity of the implant material has been one of the major hurdles in the implant technology since 2003. As mentioned earlier, the implant material triggers coagulation cascade when it comes into contact with blood. The interaction between biomedical implant and blood begins with the adsorption of plasma proteins (serum albumin, fibrinogen, *etc*.) on its surface. Initially, highly abundant proteins such as serum albumin, flbrinogen, and flbronectin are adsorbed but are later replaced by factors XII and high molecular weight kininogen. The ratio of adsorbed flbrinogen and albumin is crucial in the determination of hemocompatibility of the biomaterial. Previously, a low ratio of fibrinogen/albumin adsorbed on a biomedical implant surface has been correlated with low platelet adhesion and thrombus formation.[1] As shown in **Figure 5a**, Gr-NiTi exhibit low fibrinogen/albumin ratio relative to pristine NiTi suggesting better hemocompatibility arising from graphene. The fib/alb ratio was significantly lower for both 1 and 4 sccm Gr-NiTi indicating that the hemocompatibility of graphene is layer independent.

It is known that the electron transfer from fibrinogen molecule to the implant is responsible for the formation of fibrin as a first step to thrombus growth. As shown in **Figure 5b**, fibrinogen exhibits semi-conductor like density of electronic states or DOS (denoted by *p(E)*) with an energy gap of 1.8 eV. The Fermi levels (*EF*) of fibrinogen and Gr-NiTi equilibrate at their interface. A charge transfer of one electron per fibrinogen is required for the formation of fibrin on pristine NiTi, and electron transfer from the fibrinogen molecule into Gr-NiTi is only possible from the occupied electronic states of the fibrinogen molecule into empty electronic states of Gr-NiTi at the same energy level. Both single- and few-layer graphene are semi-metals at room temperature with a low *p(E)* in the vicinity of E_F. [24] Thus, the charge exchange current from fibrinogen to graphene is insignificant (as compared to bare nitinol) due to low values of *p(E)*. This intrinsic property of graphene coatings is crucial for inhibiting any charge transfer from fibrinogen (and subsequent blood clotting).

We employed micro-Raman spectroscopy to confirm that the charge transfer dynamics between fibrinogen and Gr-NiTi is indeed insignificant. The Raman spectrum of graphene exhibits several sharp features due to resonance effects. Notably, the tangential band (*G-band*) arises from the planar vibration of carbon atoms and was previously found to be highly sensitive to charge transfer.[25] The *G-band* frequency is known to upshift (downshift) when any acceptor (donor) species interacts with graphene *via* hole (electron) transfer. Importantly, the lineshape of the *G-band* deviates from a symmetric Lorentzian to an asymmetric Breit-Wigner-Fano (BWF) lineshape due to charge transfer.[25] As expected, we did not observe a shift in the *G-band* frequency of graphene upon adsorption of fibrinogen confirming the absence of charge transfer between Gr-NiTi and fibrinogen (**Figure 6**). Such inhibition of charge transfer and low fib/alb ratio indicate good hemocompatibility of graphene coatings.

*Chemical inertness of Graphene Coatings:*Graphene is known to act as a protection layer due to its unique physicochemical properties. Its sp^2 honeycomb lattice provides a natural diffusion barrier and therefore prevents metal ion leaching from the implant material. Recently, graphene has been used as a microscopic airtight balloon[26] and protective coating for Cu/Ni. [27] Although the stability and impermeability of graphene are well documented in the literature, we present our data related to etching of a Cu coin in **Figure 7** to reiterate the usefulness and viability of graphene as implant coatings. As shown in **Figure 7a**, the graphene coated portion of the coin (~95% Cu) remains protected from oxidation when exposed to H_2O_2 while the bare region of the coin became discolored upon contact with 5% H_2O_2 (see the magnified optical microscope image in **Figure 7a**).

To test the durability of graphene coatings, we exposed Gr-NiTi substrates to 70% nitric acid until the NiTi was partially etched away. Our *in situ* Raman spectroscopy of Gr-NiTi immersed in HNO_3 showed no change in the D- and G- band of graphene implying that the graphene coating is extremely durable (**Figure 7b**). Furthermore, we found that the graphene coating in Gr-NiTi reduces the etch rate of the underlying copper as shown in **Figure 7c**.

In conclusion, our detailed spectroscopic measurements confirmed the lack of charge transfer between graphene and fibrinogen suggesting that graphene coating inhibits platelet activation by implants. Additionally, graphene coatings do not exhibit any significant *in vitro* toxicity for endothelial and smooth muscle cell lines confirming their biocompatibility. Further, graphene coatings were found to be chemically inert, durable and impermeable in flowing blood environment. The bio- and hemocompatibility of graphene coatings along with its chemical inertness, durability and impermeability make graphene a unique material for coating biomedical implants. Lastly, we note that we succeeded in transferring graphene sheets onto individual NiTi fibers, using which the graphene-coated mesh can be manufactured. We have also developed chemically exfoliated graphene sheets that can be directly spin coated onto the mesh-like stents. In addition, our preliminary experiments show that it is indeed possible to grow graphene directly on NiTi alloy.

Disclosures

No conflicts of interest declared.

References

1. Roy, R.K. & Lee, K.-R. Biomedical applications of diamond-like carbon coatings: A review. *Journal of Biomedical Materials Research Part B-Applied Biomaterials.* **83 B** (1), 72-84 (2007).
2. Shah, A.K., Sinha, R.K., Hickok, N.J., & Tuan, R.S. High-resolution morphometric analysis of human osteoblastic cell adhesion on clinically relevant orthopedic alloys. *Bone.* **24** (5), 499-506 (1999).
3. Huang, N., Yang, P., Leng, Y.X., Chen, J.Y., Sun, H., Wang, J., Wang, G.J., Ding, P.D., Xi, T.F., & Leng, Y. Hemocompatibility of titanium oxide films. *Biomaterials.* **24** (13), 2177-2187 (2003).
4. Gutensohn, K., Beythien, C., Bau, J., Fenner, T., Grewe, P., Koester, R., Padmanaban, K., & Kuehnl, P. *In vitro* analyses of diamond-like carbon coated stents: Reduction of metal ion release, platelet activation, and thrombogenicity. *Thrombosis Research.* **99** (6), 577-585 (2000).
5. Gillespie, W.J., Frampton, C.M.A., Henderson, R.J., & Ryan, P.M. The Incidence of Cancer Following Total Hip-Replacement. *Journal of Bone and Joint Surgery-British Volume.* **70** (4), 539-542 (1988).
6. Sperling, C., Schweiss, R.B., Streller, U., & Werner, C. *In vitro* hemocompatibility of self-assembled monolayers displaying various functional groups. *Biomaterials.* **26** (33), 6547-6557 (2005).
7. Mikhalovska, L.I., Santin, M., Denyer, S.P., Lloyd, A.W., Teer, D.G., Field, S., & Mikhalovsky, S. Fibrinogen adsorption and platelet adhesion to metal and carbon coatings. *Thrombosis and Haemostasis.* **92** (5), 1032-1039 (2004).
8. Airoldi, F., Colombo, A., Tavano, D., Stankovic, G., Klugmann, S., Paolillo, V., Bonizzoni, E., Briguori, C., Carlino, M., Montorfano, M., Liistro, F., Castelli, A., Ferrari, A., Sgura, F., & Di Mario, C. Comparison of diamond-like carbon-coated stents versus uncoated stainless steel stents in coronary artery disease. *American Journal of Cardiology.* **93** (4), 474-477 (2004).
9. Allen, M., Myer, B., & Rushton, N. *In vitro* and *in vivo* investigations into the biocompatibility of diamond-like carbon (DLC) coatings for orthopedic applications. *Journal of Biomedical Materials Research.* **58** (3), 319-328 (2001).
10. Butter, R., Allen, M., Chandra, L., Lettington, A.H., & Rushton, N. *In-vitro* Studies of DLC Coatings with Silicon Intermediate Layer. *Diamond and Related Materials.* **4** (5-6), 857-861 (1995).
11. Dearnaley, G. & Arps, J.H. Biomedical applications of diamond-like carbon (DLC) coatings: A review. *Surface & Coatings Technology.* **200** (7), 2518-2524 (2005).
12. Dorner-Reisel, A., Schurer, C., Nischan, C., Seidel, O., & Muller, E. Diamond-like carbon: alteration of the biological acceptance due to Ca-O incorporation. *Thin Solid Films.* **420**, 263-268 (2002).
13. Dowling, D.P., Kola, P.V., Donnelly, K., Kelly, T.C., Brumitt, K., Lloyd, L., Eloy, R., Therin, M., & Weill, N. Evaluation of diamond-like carbon-coated orthopaedic implants. *Diamond and Related Materials.* **6** (2-4), 390-393 (1997).
14. Grill, A., Diamond-like carbon coatings as biocompatible materials - an overview. *Diamond and Related Materials.* **12** (2), 166-170 (2003).
15. Hauert, R., A review of modified DLC coatings for biological applications. *Diamond and Related Materials.* **12** (3-7), 583-589 (2003).
16. Windecker, S., Mayer, I., De Pasquale, G., Maier, W., Dirsch, O., De Groot, P., Wu, Y.P., Noll, G., Leskosek, B., Meier, B., & Hess, O.M. Working Grp Novel Surface, C., Stent coating with titanium-nitride-oxide for reduction of neointimal hyperplasia. *Circulation.* **104** (8), 928-933 (2001).
17. Zhang, F., Zheng, Z.H., Chen, Y., Liu, X.G., Chen, A.Q., & Jiang, Z.B. *In vivo* investigation of blood compatibility of titanium oxide films. *Journal of Biomedical Materials Research.* **42** (1), 128-133 (1998).
18. Bolz, A. & Schaldach, M. Artificial-Heart Valves - Improved Blood Compatibility By PECVD a-SiC-H COATING. *Artificial Organs.* **14** (4), 260-269 (1990).
19. Haude, M., Konorza, T.F.M., Kalnins, U., Erglis, A., Saunamaki, K., Glogar, H.D., Grube, E., Gil, R., Serra, A., Richardt, H.G., Sick, P., Erbel, R., & Invest, C.T. Heparin-coated stent placement for the treatment of stenoses in small coronary arteries of symptomatic patients. *Circulation.* **107** (9), 1265-1270 (2003).
20. Suggs, L.J., Shive, M.S., Garcia, C.A., Anderson, J.M., & Mikos, A.G. *In vitro* cytotoxicity and *in vivo* biocompatibility of poly(propylene fumarate-co-ethylene glycol) hydrogels. *Journal of Biomedical Materials Research.* **46** (1), 22-32 (1999).
21. Clarotti, G., Schue, F., Sledz, J., Benaoumar, A.A., Geckeler, K.E., Orsetti, A., & Paleirac, G. Modification of the biocompatible and haemocompatible properties of polymer substrates by plasma-deposited fluorocarbon coatings. *Biomaterials.* **13** (12), 832-840 (1992).
22. Gombotz, W.R., Guanghui, W., Horbett, T.A., & Hoffman, A.S. Protein adsorption to poly(ethylene oxide) surfaces. *Journal of Biomedical Materials Research.* **25** (12), 1547-1562 (1991).
23. Ishihara, K., Fukumoto, K., Iwasaki, Y., & Nakabayashi, N. Modification of polysulfone with phospholipid polymer for improvement of the blood compatibility. Part 2. Protein adsorption and platelet adhesion. *Biomaterials.* **20** (17), 1553-1559 (1999).
24. Jung, N., Kim, B., Crowther, A.C., Kim, N., Nuckolls, C., & Brus, L. Optical Reflectivity and Raman Scattering in Few-Layer-Thick Graphene Highly Doped by K and Rb. *ACS Nano.* **5** (7), 5708-16 (2011).
25. Rao, A.M., Eklund, P.C., Bandow, S., Thess, A., & Smalley, R.E. Evidence for charge transfer in doped carbon nanotube bundles from Raman scattering. *Nature.* **388** (6639), 257-259 (1997).
26. Bunch, J.S., Verbridge, S.S., Alden, J.S., van der Zande, A.M., Parpia, J.M., Craighead, H.G., & McEuen, P.L. Impermeable atomic membranes from graphene sheets. *Nano Letters.* **8** (8), 2458-2462 (2008).
27. Chen, S., Brown, L., Levendorf, M., Cai, W., Ju, S.-Y., Edgeworth, J., Li, X., Magnuson, C.W., Velamakanni, A., Piner, R.D., Kang, J., Park, J., & Ruoff, R.S. Oxidation Resistance of Graphene-Coated Cu and Cu/Ni Alloy. *Acs Nano.* **5** (2), 1321-1327 (2011).

